Active Damping, Inertial Electro-Mechanical Ballscrew Actuator

MATTEUZZI Nicola
NARDESCHI Marco
TORO Stefano
Umbra Cuscinetti SpA,
ZI Località Paciana
06034 Foligno PG, Italy

COLOGNI Alberto
MADASCHI Matteo
PREVIDI Fabio
Università degli Studi di Bergamo,
Via Marconi 5
24044 Dalmine BG, Italy

SAVARESI Sergio
Politecnico di Milano,
P.zza Leonardo da Vinci 32
20133 Milano, Italy

ABSTRACT

The damping of vibrations on aircrafts and rotorcrafts can provide life extension or weight reduction on those structures on which the vibration load is a significant amount of load endurance spectrum. A hybrid active-passive inertial actuator system is presented focusing the advantages of a ballscrew based actuator and of a non-conventional three phase control drive.
The dynamics of the mechanical system, of the electric motor and of the associated electronic control unit has been simulated as an integrated system on a MatLab/Simulink® platform. The design of the damper has been finalized by simulation, including full three-phase bridge drive with independent phases (no star-point) and motor control law and mechanics and elasticity of the system. The test results on a full-scale prototype of the damper are presented.

KEYWORDS

Active Damping, Ballscrew, Inertial Actuator, Vibration

INTRODUCTION

The approaches for control of vibrations are usually divided into two categories: passive damping and active damping. Examples of passive damping materials include viscoelastic materials (VEMs), viscous fluids, magnets, smart materials (piezo-ceramics, electro-rheological fluids, magneto-rheological fluids, magneto-restrictives, shape memory alloys), high damping alloys, and particle damping. These systems use the potential energy generated by the structural response to provide the control force. The most common of these is viscoelastic materials. VEMs dissipate mechanical energy into heat when they undergo cyclic stress due to polymer chain interactions [Sun 1995]. Active damping is sometimes necessary to achieve greater performance, or to produce controlled system properties. Due to their lack of versatility, passive vibration damping strategies become ineffective when the dynamics of the system or the frequencies of the disturbance vary with time. Additionally, active systems can provide increased effectiveness in controlling vibration compared to passive approaches. Active damping systems require sensors and actuators, a source of power, and a control system [Vahdati 1993]. Another useful strategy to control vibration is by the dynamic response of a specifically tuned mass that instead of dissipating the energy of vibration, absorbs such energy by oscillation, in such a way to prevent vibration force transmission to the structures [Den Hartog 2013].
All these strategies can be combined together in order to provide a vibration control system with enhanced performance with respect to bandwidth, power required, thermal management, etc. A system based on an active electromechanical system has been designed and developed. The EMA design is of DD (i.e. direct drive) type: it means no gears are interposed between the electric motor and the ballscrew assy (*Figure 1)*.
The ballscrew is of the rotating screw-translating nut type. The actuation is provided by a permanent magnet brushless motor, directly connected to the screwshaft. The output force of the actuator is measured by a load-cell on top of the connection rod-end, and linked to a flexible structure.
The purpose of the system is to damp the vibrations generated by a vibration of the structure, in order to minimize (nullify) the vibration of the oscillating mass.
This concept can be used in a variety of applications, for instance the vibration of the struts connecting an engine to the nacelle or the vibration generated by a propeller on the

attachment of the gearbox to the structures [Henderson 2012].

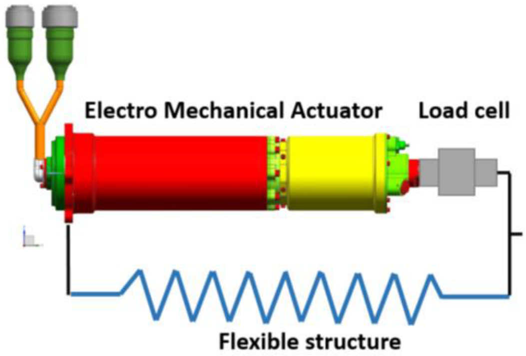

Figure 1

MECHANICS

The classic dynamic vibration absorber is a simple system where an absorber mass is connected to an undamped main mass-spring system, and tuned to the resonant frequency of the main mass and spring. When a force with the same frequency of the tuned frequency of the absorber system is applied, no motion of the main mass results and no net reaction force (other than static equilibrium force) is required at the constraint *(Figure 2)*.

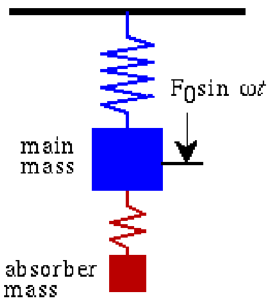

Figure 2

To this simple classical concept we can add a sensor and an actuator with the result of being able to damp a higher bandwidth with little power effort (Figure 3).
The system of second order ODE that models the damper is derived by the simple equation of motions of the lumped parameter model. The equations have been derived by the classical approach of the ballscrew joint that can be assumed to be an infinite wedge with angle α *(Figure 4)*.
The equivalence of the rotating motion to a translating motion is completed by the equivalence of a moment of inertia to a linear inertia

$$m_{eq} = \frac{4\pi^2 J}{p^2} \qquad (1)$$

$$m\,\ddot{x}_m = k_S(x_i - x_m) + k_{eq}(x_v + y_v \tan\alpha - x_m) + c_S(\dot{x}_i - \dot{x}_m) + c_c(\dot{x}_v + \dot{y}_v \tan\alpha - \dot{x}_m) \qquad (2)$$

$$m_v\,\ddot{x}_v = k_v(x_i - x_v) - k_{eq}(x_v + y_v \tan\alpha - x_m) + c_v(\dot{x}_i - \dot{x}_v) - c_c(\dot{x}_v + \dot{y}_v \tan\alpha - \dot{x}_m) \qquad (3)$$

$$m_{eq}\,\ddot{y}_v \tan\alpha = -k_{eq}(x_v + y_v \tan\alpha - x_m) - c_c(\dot{x}_v + \dot{y}_v \tan\alpha - \dot{x}_m) \qquad (4)$$

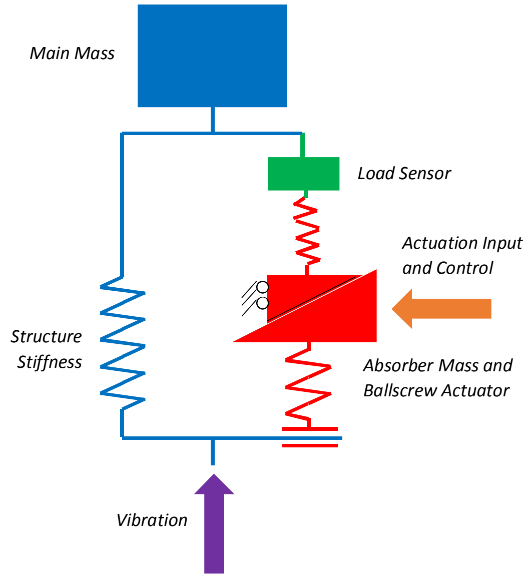

Figure 3

Where

$$k_{eq} = \frac{k_c \cdot k_{LC}}{k_c + k_{LC}} \qquad (5)$$

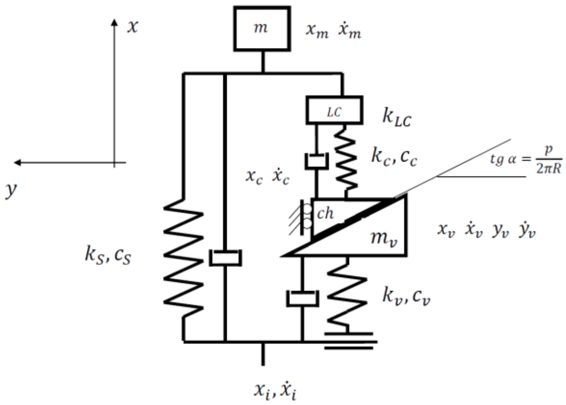

Figure 4

The study of the system state space response validates the principle of vibration damping in the neighborhood of a resonant frequency that can be tuned by a proper design choice of the ballscrew pitch and actuator stiffness.
The indicated response of x_m versus x_i shows the dynamic damping of the input vibration on the oscillating main mass, corresponding to the natural frequency of the actuator mass and overall stiffness *(Figure 5)*.
The blue line is for an undamped system, the grey line is the same system with structural damping.
Although the overall mechanical dynamic behavior of the system can be efficiently studied with the analytical ODE

model based on the previous equations, in order to have a complete simulation of the whole electro-mechanical system the MatLab/Simulink® platform has been used.

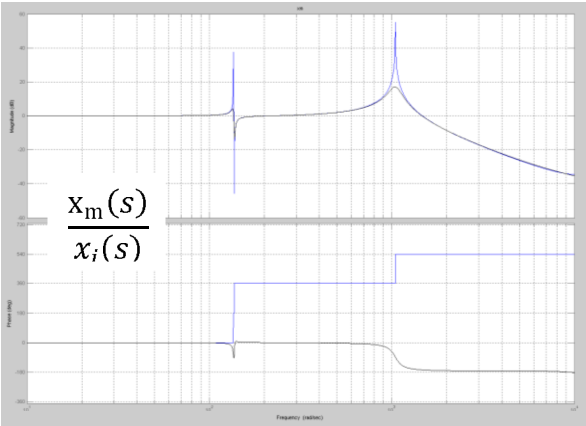

Figure 5

The lumped parameters model includes mechanics, electric motor, associated electronic control unit (i.e. full three-phase bridge drive with independent phases) and related motor control laws (*Figure 6*). Results are not reported for limitation of space.

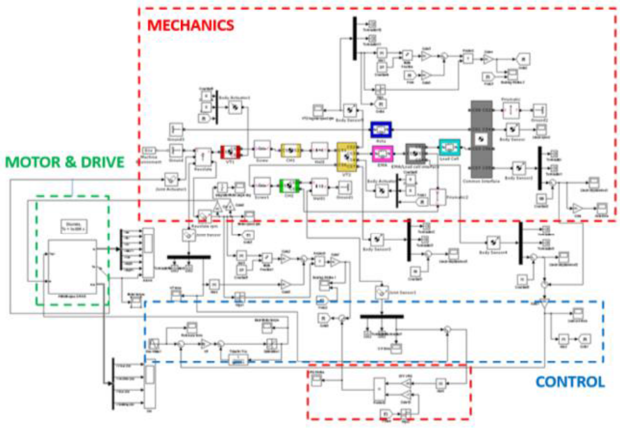

Figure 6

ACTUATOR REQUIREMENTS

The EMA main requirement is to provide a sinusoidal force, F, with a variable amplitude between 0 and F_{max}, at a specific working frequency f_w. The external load is basically of elastic nature and represented by the stiffness of the flexible structure where the actuator is assembled in *(Figure 7)*.

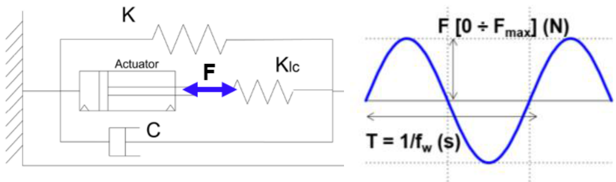

Figure 7

ELECTRONIC DRIVE AND CONTROL

The control system is based on two nested control loops. The inner one is the current control systems. The second one is a speed or force controller. In this paper, an original current control algorithm for multilevel inverters is presented.

In order to drive the system, a multilevel electronic inverter has been designed. Multilevel inverters are preferred in high power medium-voltage energy control applications, due to their high voltage capability, reduced Common Mode Voltages, nearly sinusoidal output voltage and power quality associated with reduced harmonic distortion and lower electromagnetic interferences (EMI). They can have increased output voltage amplitude with respect to standard inverters and they can reduce the current harmonic content and the switching frequency to which the switches are subjected. The two most popular techniques for the generation of PWM in multilevel inverters are sine-triangle PWM (SPWM) and Space Vector PWM (SVPWM). SPWM involves the comparison of a reference signal with a number of level shifted carriers to generate the PWM signal. SVPWM involves synthesizing the reference voltage space vector by switching among the three nearest voltage space vectors. Several SVPWM techniques have been discussed extensively in literature [Celanovic 2011], [Gupta 2006] and [Van Den Broeck 1988]. The PWM techniques complexity and computational cost increase with the number of levels of the inverter.

The schematic diagram of an open-end winding brushless motor drive inverter is shown in *(Figure 8*

.

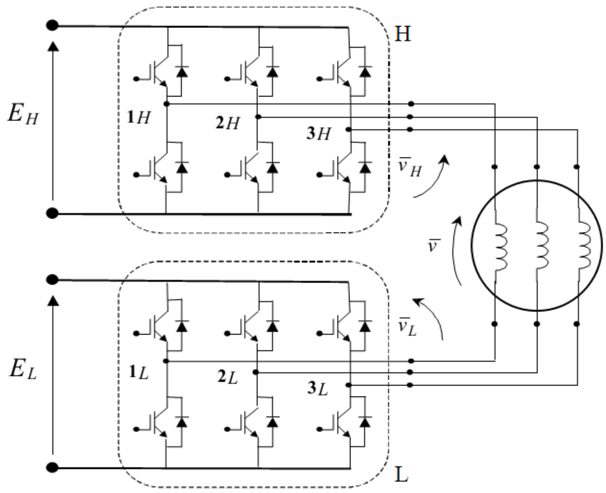

Figure 8

The combination of the eight switch configurations for each two level inverter yields 64 possible switches states for the whole multilevel converter, corresponding to 18 different output voltage vectors and a null vector and 24 sectors, as represented in *(Figure 9)*.
By using the SVM technique, these voltage vectors can be combined to obtain any output voltage vector lying inside the outer hexagon.

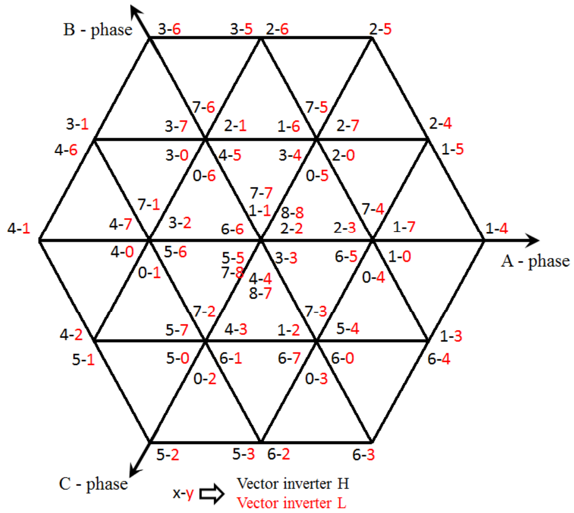

Figure 9

To achieve this purpose it's necessary to study in depth the space of vectors *(Figure 10)*. It is possible to notice that the hexagon of the resultant space vectors combination can be created using only some combinations and not all of them. Hence this work will be focused on simplifying the number of combinations and use them efficiently.

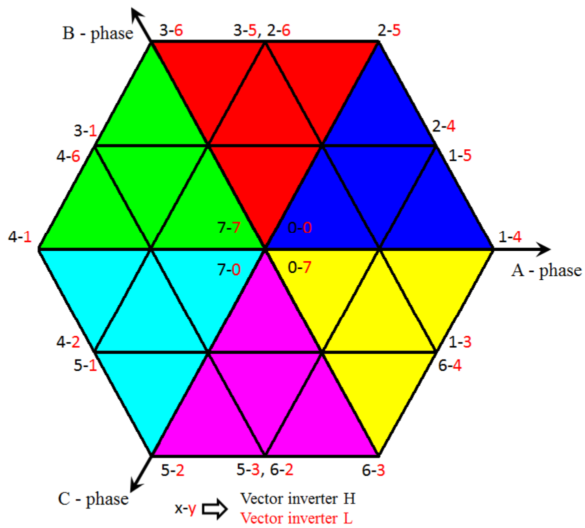

Figure 10

In fact, it is possible to use a standard SVM, for motors with star connection, for each inverters.
The sectors 1, 7, 8 and 9 are contained by four combinations *{1,4}*, *{2,4}*, *{1,5}* and *{2,5}*, and these sectors can be seen as a macro sector 1 where for the inverter *H* the active space vectors are *U1* and *U2* while for inverter *L* the active space vectors are *U4* and *U5*, that are the opposite space vectors with respect to the ones of inverter 1. The combinations for the other macro sectors are very simple to deduce *(Figure 10)*.
Therefore, in order to apply these couples of space vectors, it is necessary to be sure that inverter *L* computes always the opposite space vectors of inverter *H*. To do this, it is enough to use standard SVM, but feeding it with negated signals: in this way, when the SVM standard of inverter *H* calculates the PWMs for sector I, the inverter *L* calculates the PWMs for sector IV.
In this way the generation of PWMs is very simple, since it is possible to reuse the standard SVM, provided that some constraints are fulfilled. Finally, to control efficiently the current, it is necessary to use the completed Clarke and Park transform because the system is not balanced. In *(Figure 11)*, the current loop control scheme for the motors with open-end windings is shown [Madaschi 2013]. Direct and quadrature currents are regulated by means of PI controllers.

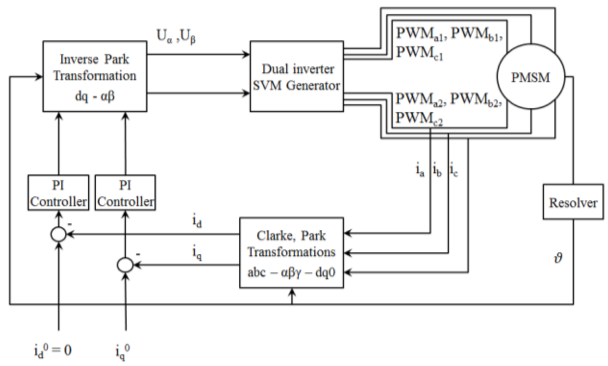

Figure 11

TEST RESULTS

A specific test actuator *(Figure 12)* and electronic control unit *(Figure 13)* has been realized in order to verify all actuator performances, in terms of generated force, kinematic parameters (angular and linear displacement/velocity/acceleration) and current/power absorption.

Figure 12

The related test rig control software has been designed in order to accept one of the following inputs:
- a single sinusoidal quadrature current reference signal (open loop force mode);
- a single sinusoidal force reference signal (closed loop force mode);
- a frequency sweep with a fixed amplitude quadrature current reference signal.

Figure 13

Results are shown in terms of normalized parameters: specifically developed force has been normalized to maximum force amplitude, quadrature current to current sensors full-scale and frequency to design working frequency.

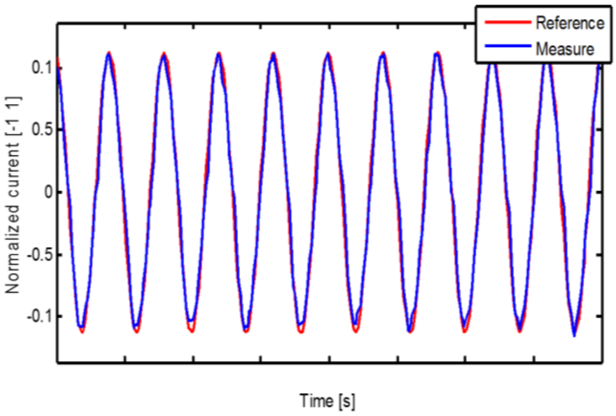

Figure 14

The quadrature current (which is directly related to the torque generation) is perfectly in phase and the controller ensures good quality tracking of the reference *(Figure 14)*. The direct current is close to the commanded value zero with very small oscillations *(Figure 15)*. As expected the rotor position is perfectly in phase with the quadrature current *(Figure 16)*. In order to test the effective efficiency of the overall system a simple and linear force regulator has been implemented. The effectiveness of force controller at working frequency is shown *(Figure 17)* and *(Figure 18)*.
Reference force is plotted versus measured force *(Figure 17)*: the force controller succeeds in following the requested force. The comparison between the commanded quadrature current and the current measured within current controller is reported *(Figure 18)*.

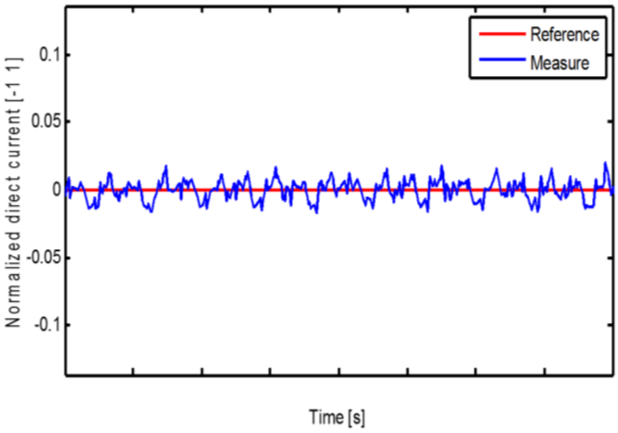

Figure 15

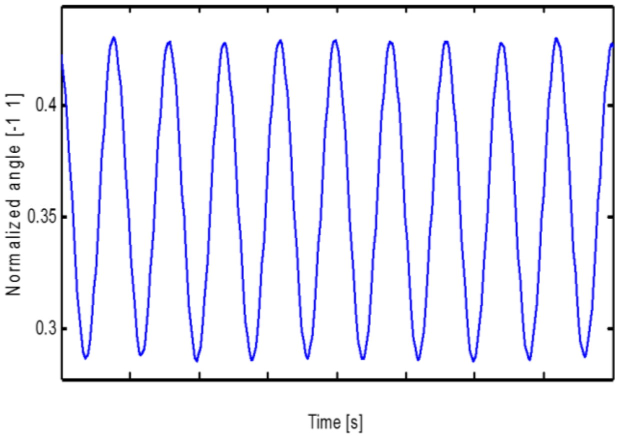

Figure 16

As expected the EMA highlights a perfect linear behavior in terms of relationship among quadrature current, screwshaft angular position and developed force within all requested force range. The developed force is linear with the quadrature current *(Figure 19)*.

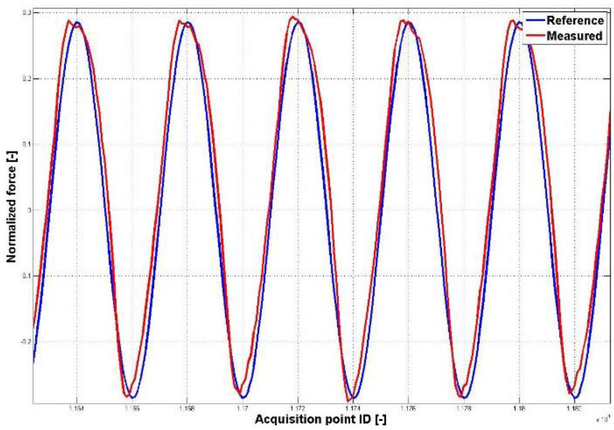

Figure 17

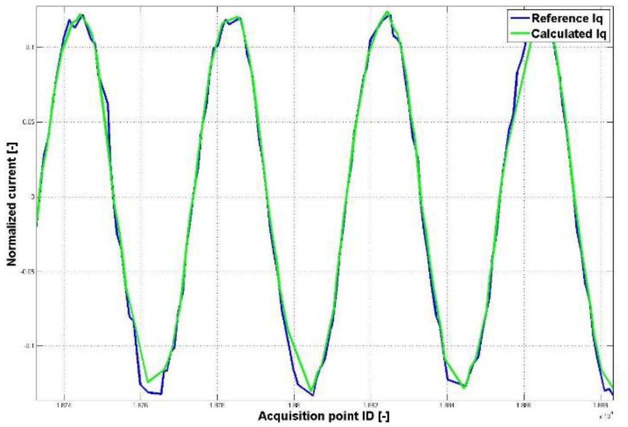

Figure 18

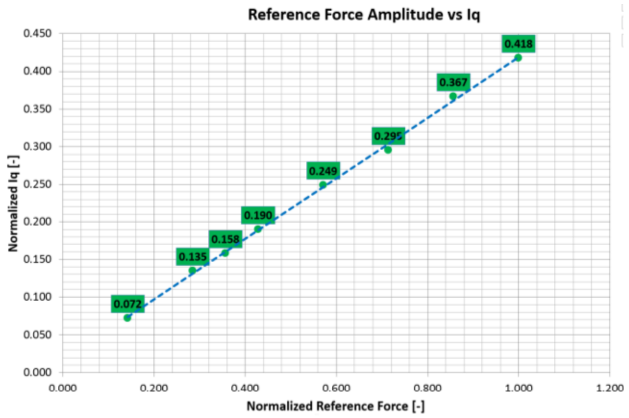

Figure 19

Wide current controller bandwidth has permitted to perform a frequency characterization of the EMA. In particular a fixed amplitude frequency sweep for quadrature current has been set as input with a frequency range up to 2.4 times the design working frequency. Measured force amplitude is not constant over the frequency range *(Figure 20)*, showing an amplification peak of 2.1 in correspondence of a specific frequency (1.88 times the design working frequency).

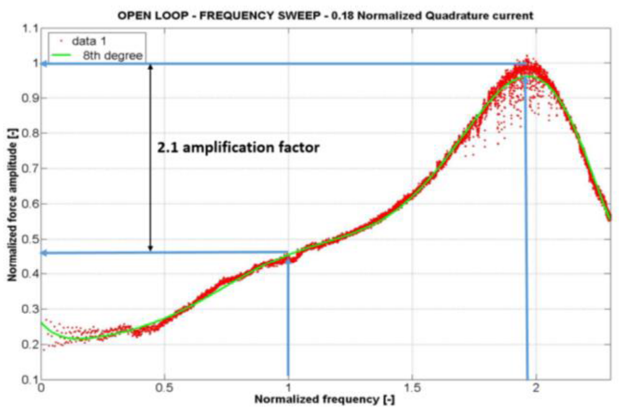

Figure 20

This frequency corresponds to the resonance frequency of the equivalent 1 DOF mass-spring-damper mechanical system which the EMA can be modelled with. Even if with a different frequency, the force target has been reached with the same quadrature current supply which provides 50% of the maximum force at the design working frequency.

ACTUATOR PERFORMANCE

The following table summarizes the main actuator performances. Confidentiality reasons do not allow to explicit the design working frequency, the maximum force amplitude and motor currents.

Electro - Mechanical Actuator	
Outside diameter	80 mm
Length	350mm
Weight	6.5 kg
Electronic control Unit	
L x W x H	5 dm^3
Weight	3 kg
Mechanical and Electrical Data	
Overall efficiency	>80%
BUS voltage	28 VDC
Installed power	750 W

Table 1

An aspect of the actuation worth mentioning is the energy flow between actuator and structure: the phase in which the actuator is compressing or extending the structural spring alternates to a phase in which the elastic energy stored in the spring is released to the actuator (regenerating phase). This phase could be used to store energy (converted from mechanical into electrical by the motor acting as a generator) in any storage device.

CONCLUSIONS

The principle of vibration damping through a ballscrew electromechanical actuator has been validated.
The advantage in terms of installed power and required current to deliver the needed force at a specified frequency can be of the order of one half, with proper design of ballscrew parameters and actuator stiffness.
A three phase motor with no star-point has been designed and built, with 70% more power available with same voltage and current supply, with respect to a traditional Y-connected motor.
A novel drive control logic has been developed in order to actuate this motor. Due to high frequency requirements, the computation of PWM control has been optimized and verified.
Linearity of the actuator has been validated on a high range of frequencies and forces.
Further investigations will be dedicated to the regenerative aspects of elastic energy stored in the structure during motoring phase of the actuator and released by the structure to the actuator during the aiding phase.

REFERENCES

Sun J. Q., Jolly M. R., Norris, M. A. (1995), "Passive, Adaptive and Active Tuned Vibration Absorbers—A Survey", *Journal of Mechanical Design June 1, 117(B) pp. 234-242, 1995.*

Vahdati N., Pike J.A. (1993), "Analytical Comparison of Active Versus Passive Aircraft Engine Suspensions", *Second Conference on Recent Advances in Active Control of Sound and Vibration, Blacksburg, VA*.

Den Hartog, J. P. (2013). "Mechanical vibrations", *Courier Dover Publications.*

Henderson J. P., Plummer A., Johnston N. (2012), "Hybrid Active-Passive Electro-Hydrostatic Vibration Isolation for Rotorcraft", *Proc. of Recent Advances in Aerospace Actuation Systems and Components, pp. 44-50, Toulouse, 2012.*

Celanovic N., Boroyevich D., Skudelny H. C. and Stanke G. V. (2011), "A fast Space Vector Modulation algorithm for multilevel three-phase converters", *in IEEE Transaction on Industry Application Vol.37, No. 2, pp. 637 - 641 March/April 2011.*

Gupta A. K. and Khambadkone A. (2006), "A Space Vector PWM Scheme for Multilevel Inverters Based on Two-Level Space Vector PWM", *in IEEE Transaction on Industrial Electronics Vol.53, No. 5, pp. 1631-1639, October 2006.*

Van Den Broeck H. W., Skudelny H. C. and Stanke G. V. (1988), "Analysis and Realization of a Pulsewidth Modulator Based on Voltage Space Vectors", *in IEEE Transaction on Industry Application Vol. 24, No. 1, pp. 142-150, January/February 1988.*

Madaschi M. G., Gryazina E., Cologni A. L., Spelta C., Previdi F., Savaresi S. M. and Pesenti I. (2013), "Robust control of magnetic guidance lightweight AGVs path tracking using randomization methods", *in Proc. of European Control Conference, pp. 262-267, Zurich, 2013.*